

Interferometric Evanescent Wave Biosensor Principles and Parameters

Moisi Xhoxhi¹, Alma Dudia², Aurel Ymeti³

¹Department of Engineering Physics, Faculty of Engineering Mathematics and Engineering Physics,
Polytechnic University of Tirana, Street "Muhamet Gjollësja", Tirana, Albania

^{2,3} Nanoalmyona BV, Heutinkstraat 463, 7535 AZ Enschede, The Netherlands

Abstract: This review tries to present an overview of the most important parameters to be taken in consideration in the evaluation of interferometer biosensors. Waveguide interferometers have particular importance, because by utilizing the combination of two very sensitive methods, the waveguiding and the interferometry techniques, they offer very good reliability and possibility for miniaturization and integration in optical chips. By using the evanescent wave technology they measure the interaction between receptors and biomolecules in real time without using labels. Receptors are immobilized onto a sensor surface and the interaction with the biomolecules near it cause a refractive index change. A large number of applications in life sciences, including binding kinetics of receptor-biomolecule pairs and virus-protein interactions, are using evanescent wave-based biosensors for their studies. This article describes the technology behind their sensing techniques, and a range of applications where they are used.

I. Introduction

The first biosensor is considered the enzyme electrode transducer developed by Updike and Hicks [1]. Its working principle served as the base for the many other biosensors developed so far. Almost all of them incorporate a sensitive biorecognition layer and a physicochemical transducer, which converts a biochemical signal to an electronic or optical signal, as shown in **Error! Reference source not found..** The recent developments in nanotechnology have improved the quality of biorecognition elements used in biosensors, which are typically synthesized in a laboratory. Nowadays the most popular biosensor is the one detecting the glucose concentration in blood, due to the wide spread of diabetes in developed countries [2]. The glucose monitoring technology has been improving for almost thirty years now, and as result people today can monitor their diabetes with small, fast, cheap and easy to use glucose biosensors [3].

Many other biosensing devices have been developed so far, using metal oxide semiconductor technology (CMOS), which are used in biomedical applications such as pregnancy, bacterial infection, cholesterol and troponin T quick tests [4].

The detection using the traditional methods, like PCR and ELISA, are still popular today because they are very selective and reliable, but gradually nowadays they are becoming too slow. Optical biosensor technology promises equally reliable results but in much shorter time, and their potential market is very encouraging. However, their cost and complexity is a drawback and much work needs to be done in order for them to become a real alternative. Biosensors need to show that they are capable of reaching at least the same detection levels as traditional techniques,

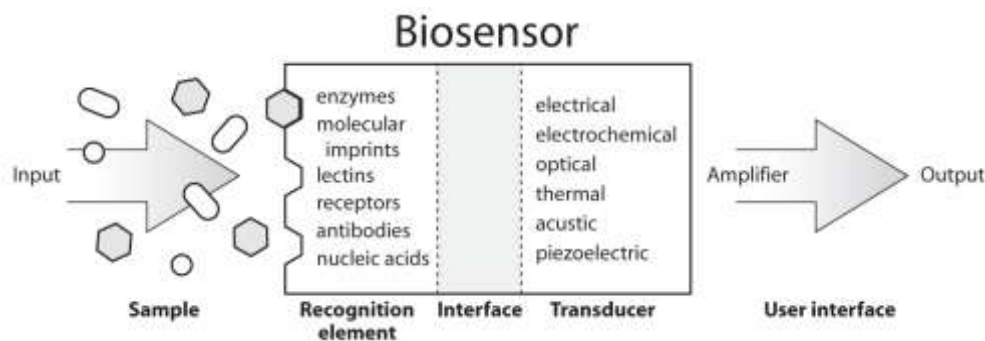


Fig. 1 Biorecognition and transduction layer elements in a biosensor design (Chambers et al., 2008). Reprinted from "Biosensor Recognition Elements" by J. P. Chambers, B. P. Arulanandam, L. L. Matta, A. Weis and J. J. Valdes, 2008, *Current Issues in Molecular Biology*, 10, p. 1. Copyright 2008 by Horizon Scientific Press.

but with a lower cost [5, 6]. Improving metrics such as sensitivity, cost, and ease of use of a biosensor can have a big impact on their commercial success [7]. Electrochemical techniques generally classified according to the observed parameter: current (amperometric), potential (potentiometric) or impedance (impedimetric) offer lower cost but these techniques present more limited selectivity and sensitivity than their optical counterparts [8].

Detecting the biological analytes directly through their physical properties (such as mass, size or electrical impedance) presents many difficulties, therefore scientists have been using some sort of “label” (mainly fluorescent or magnetic substances) which attach to the molecules, viruses or cells being studied. The label indirectly indicates the presence of the analyte to which it has been attached by identifying its color or detecting the photons generated at a particular wavelength [9, 10]. However, although the use of labels gives a very good sensitivity, their usage causes many other side effects. In general, this treatment results in the death of the specimen, which prevents the ability to study a single population repeatedly over a long time. Also, the use of labels requires special labs and large quantities of reagents and equipments that must be properly disposed. The loss of color of the fluorescent chemical compound over time due to exposure to light reduces the ability of this technique to supply measurements in high quantity. In case when nanoparticles are used as labels, their use requires a high degree of development to assure that the label does not block the attached molecule or modify its shape or structure [7]. The hydrophobic nature of fluorescent compounds used in labeling makes them have a tendency to form clusters in the solution, creating background binding which is a significant problem leading to errors in detection [11]. The interaction strength between the target molecule and receptor is indicated by the intensity of the fluorescence. The signal generated by the fluorescent substance and the fact that the number of fluorophores on each molecule cannot be precisely controlled, makes it difficult to make a quantitative analysis [12]. Due to these disadvantages, there has been a drive to develop methods that allow direct detection of biological analytes without labels, which would reduce cost and complexity while providing more quantitative information.

By detecting analytes in their natural form, label-free detection removes the experimental uncertainty induced by the effect of the label and in general it measures the refractive index change (RI) induced by molecular interactions. The RI change is related to the sample concentration, while the detection signal usually depends on the total number of analytes in the volume. As a result, the detection signal does not scale down with the sample volume. This characteristic makes label-free detection advantageous over label-based detection and particularly attractive when ultra small (femtoliter to nanoliter) detection volume is involved [12].

One way of label-free sensing is by using optical techniques, where in general an optical waveguide confines an electromagnetic wave in such a way that it can interact with a test sample. The electromagnetic wave may be a traveling or a standing wave, depending on the sensor configuration, but in both cases the structure must be designed so that the extending wave from the waveguide surface can penetrate into the test sample. This extending wave has an exponential decay in its intensity and is called the *evanescent field*. Back in 1970s, evanescent waves were used to study ultra-thin metal films and coatings [11]. The evanescent field extends only ~100–150 nm into the test sample for the typical wavelength range for optical biosensors (600–900 nm), therefore it can make a good discrimination between the analyte attached to the receptor near the surface and the unbound material suspended in the solution. One key to high sensitivity sensor design is to match the regions of greatest biochemical binding to those with the highest evanescent field intensity [7].

In evanescent field based detection the biomolecular interaction affects the guiding properties of the waveguide due to the change in refractive index. The change in refractive index can then be evaluated by the optical properties of the waveguide such as intensity, phase, polarization, etc, which can then be correlated with the concentration of the analyte, resulting in a quantitative value of the interaction [13]. Biosensors based on evanescent field detection have shown to be very good candidates for point of care devices due to their extreme sensitivity for label-free and real-time sensing. Their detection limit is close to 10^{-7} - 10^{-8} in bulk refractive index. Other evanescent field biosensors are those using Surface Plasmon Resonance (SPR), which is based on the variation of the reflectivity on a metallic layer in close contact with a dielectric media. Their sensitivity goes to 10^{-5} – 10^{-7} RIU in bulk and 1-5 pg/mm^2 in surface, but one drawback of SPR sensors is that they have a relatively large size making their integration in Lab-on-Chip (LOC) platforms difficult. Today, the few commercialized IO biosensors present on the market are expensive and not truly portable. Many progresses have been done in this direction due to advances in silicon technology but there are still limitations in the integration of all the components into one single system [14].

The main advantage of evanescent based mechanism is that it is not necessary to separate in advance the nonspecific components because any change in the bulk solution will hardly affect the sensor response. Therefore, the evanescent field mechanism is very useful for label-free detection of analytes or biochemical reactions in complex real samples. The major contributing factor to the sensitivity of a system is the strength of light-matter interaction. For a sensing system the smallest amount of analyte that produces a measurable output signal is defined as the *detection limit* (DL) for that system. It can be specified in two main ways: a) according

to the changes in the bulk refractive index of the solution above the sensor surface (expressed as refractive index units (RIU)); b) according to the surface sensitivity, related to the accumulation of mass on the sensor surface, normally expressed as surface mass density (pg/mm^2). The best resolutions for bulk refractive index changes are within the range of 10^{-7} to 10^{-8} RIU, which depending on the analyte and transducer mechanism means that concentrations down to ng/ml or pg/ml can be determined [13].

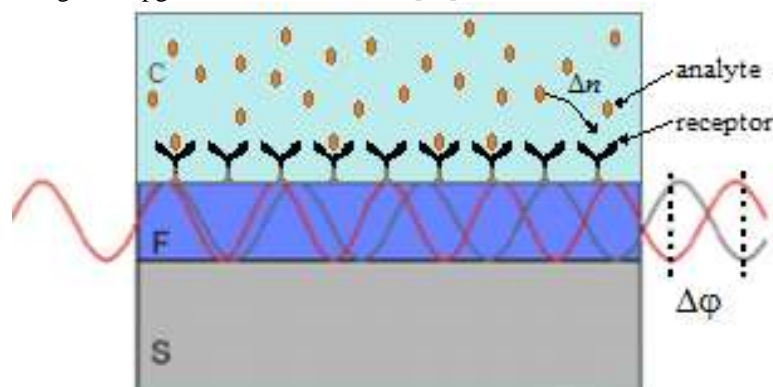


Fig. 2 Schematic working principle of a planar waveguide interferometer. The binding of analyte to the receptors causes a refractive index change near the surface, Δn . This change induces a phase shift, $\Delta\phi$, of the signal in the measuring channel relative to the reference one, which is measured based on their interference.

On the other hand waveguide interferometers lack some specific features and have some drawbacks compared to the other sensors. One of them is that only relative parameter values (related to a reference) can be gained from a waveguide interferometer. Additionally, they are highly sensitive for wavelength instabilities. Consequently, temperature stabilized light sources need to be applied in order to avoid wrong interpretation of the measurement. Furthermore, in order to suppress the non-negligible effects of mechanical vibrations and temperature changes, the sensor unit has to be stabilized and properly isolated from the environment. The future challenge is to design waveguide interferometer sensor systems, which are capable of detecting and investigating bio-chemical reactions with improved sensitivity and detection limit, without the aforementioned disadvantages, and suitable for point-of-care applications.

II. Theory of planar optical waveguide interferometers

2.1 Principles of optical interferometry

The interference phenomenon first studied by Isaac Newton, who observed the interference fringes in the form of concentric rings formed from a light source after passing a plano-convex lens, could not be explained by simply regarding light as rays that propagate along straight lines. English physicist Thomas Young explained Newton's rings as an interference phenomenon, which is a characteristic of waves. His double-slit experiment in 1804 [15], was an undeniable fact and very important in accepting the wave theory of light at that time. Based on this phenomenon four basic interferometers were developed which find usage in biosensing. Michelson, Fabry-Perot, Mach-Zehnder, and Young interferometer [16]. These devices use optical interferometry for measuring small changes that occur in an optical beam along its path of propagation. Michelson interferometer finds a lot of use in infrared spectrometry for spectral identification of a compound structure [17]. It divides a beam of light into two different paths and then recombines them after introducing a difference in the two paths. As the difference in path length changes, the interference creates variations in output intensity. The intensity variations can be measured with a detector as a function of the path difference. The Fabry-Perot interferometer known also as the *etalon* is widely used in telecommunication, lasers and spectroscopy to control and measure the wavelength of light [18]. It uses a resonant cavity formed by placing two mirrors facing each other and provides very long path lengths as light bounces back and forth in the mirrors thousands of times. Long optical path designs allow very sensitive measurements of the absorption and refractive properties of a compound. Nevertheless, these configurations have found limited application in sensors due to the fact that they need prior reference measurements to be taken with an empty cavity and the moving mirrors introduce some additional complexity [19].

A practical sensor would have no moving parts, making it simple to implement, and would be able to make real-time monitoring. These features are offered from Mach-Zehnder and Young interferometers which have a wider use in biochemical measurements.

2.2. Young and Mach-Zehnder interferometer

In Young interferometer (YI) [20] and Mach-Zehnder interferometer (MZI) [21] the polarized input beam splits and propagates in different arms. In the sensor arm the beam interacts with the sample of interest,

while on the other, called the reference arm, the beam may be insulated from the environment or interacts with a reference sample. When a change happens in the sample it shifts the phase of the beam in the sensor arm compared to the one in the reference arm. In MZI the beams are recombined again in the same channel towards the photodetector, while in YI the output beams propagate in free space until they overlap and form an interference pattern on a CCD camera, as shown in figure 3.

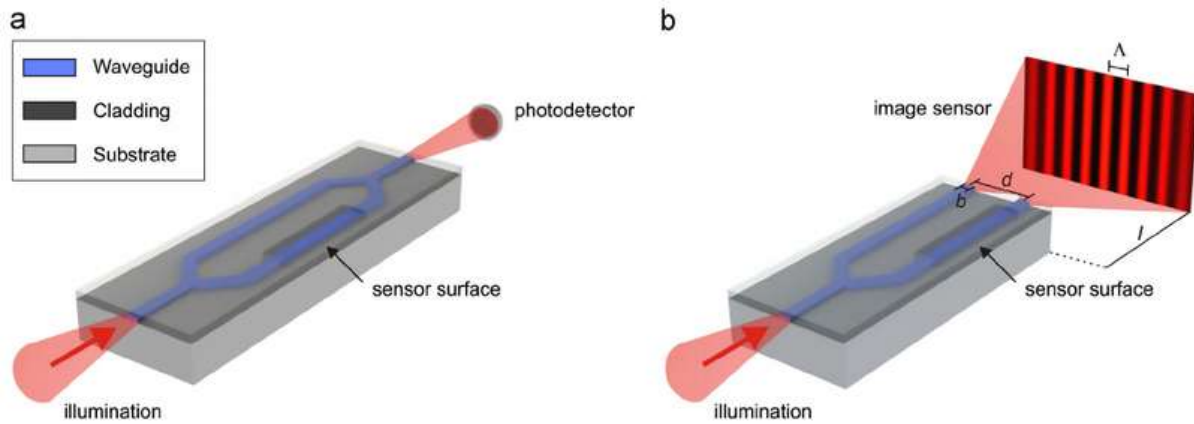


Fig 3. Typical (a) Mach-Zehnder Interferometer (MZI) and (b) Young Interferometer (YI) configurations. Reprinted from “Integrated planar optical waveguide interferometer biosensors: A comparative review” by P. Kozma, F. Kehl, E. Förster, C. Stamm, F.F. Bier, 2014, *Biosensors and Bioelectronics*, 58, p. 291. Copyright 2014 by Elsevier B.V.

In MZI the measured intensity, I , is a periodic function of the phase shift difference, $\Delta\Phi$, between the beams.

$$I = I_1 + I_2 + 2\sqrt{I_1 I_2} \cos(\Delta\Phi) \quad (2.1)$$

The phase shift difference between the two beams traveling in two different paths, L_1 and L_2 , can be calculated as [22]:

$$\Delta\Phi = k_0 \left(\int_{L_1} n(r) dr - \int_{L_2} n(r) dr \right) \quad (2.2)$$

where $k_0 = 2\pi/\lambda_0$ and λ_0 are the wavenumber and the wavelength in free space, while $n(r)$ is the refractive index of the medium at point r .

In YI the optical path length of output beams varies in the y axis, therefore the intensity of the resulting interference pattern can be calculated as [23]:

$$I(y) = \gamma(y) I_1 + I_2 + 2\sqrt{I_1 I_2} \cos(ky + \Delta\Phi) \quad (2.3)$$

where $\Lambda = l/kd$ is the spatial period of the fringes, $k = k_0 n = 2\pi/\lambda$ is the wavenumber of the medium, d the spacing between the channels, while l is the distance between output plane and the detector. The coefficient $\gamma(y)$ represents the diffraction on a single slit of width b , which modulates the intensities of the interference fringes. The difference between these two approaches lies in the fact that in MZI the intensity is related to the phase difference of the two beams, while in YI the position of the interference fringes is proportional to the phase difference of the beams.

A well known integrated MZI structure used in opto-chemical sensing which offers very high sensitivity is described in [24], while an ultrasensitive application of an integrated optical Young interferometer used for the real-time direct detection of viruses is reported in [25]. The sensitivity of this sensor is high enough to detect the presence of a single virus particle and represents a device of unprecedented sensitivity with a wide range of applications. Recently, a multichannel interferometer design based on MMI couplers is under development, which has a working principle similar to integrated optical Young interferometer, but offers a smaller footprint and more measuring channels [26].

2.3. Wave propagation in planar optical waveguides

The phenomenon of total internal reflection used today for guiding the light in a waveguide was first demonstrated by Daniel Colladon with his ‘light fountain’ experiment in 1841 and then by John Tyndall in 1854

[27, 28], where light remained confined to a falling stream of water. This phenomenon was later used in many applications, such as in telecommunication and sensor devices for the confinement and guidance of electromagnetic waves with high efficiency. The telecommunication industry developed novel methods to couple and transfer light in optical waveguides for high speed communication, while the semiconductor industry developed technologies for the fabrication of complex integrated optical (IO) systems [29]. A simple waveguide consists of three layers: a) a cover (C), b) a film (F) and c) a substrate (S), with refractive indices n_C , n_F , and n_S , respectively. In order for the light to be guided, the total internal reflection condition must be met, as shown in **Error! Reference source not found..** The refractive index of the film must be higher than that of the cover and substrate ($n_C < n_F > n_S$), and the angle of propagation relative to the interface normal must be larger than the critical angle, θ_C , at the two boundaries. Based on Snell's law the critical angle is measured as $\theta_C = \arcsin(n_{S,C}/n_F)$ [30].

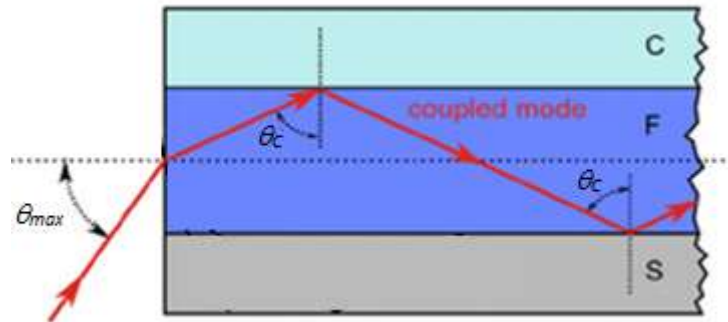


Fig 4. Light propagation in a planar optical waveguide. Light can be coupled and guided in a waveguide if $n_C < n_F > n_S$ and if the angle of light propagation relative to the interface normal is larger than the critical angle θ_C .

In order for a wave to be guided in a waveguide it must fulfill the so-called *self-consistency* (also known as *transverse resonance*) condition, whereby as the wave reflects from the boundaries it must reproduce itself by constructive interference. In short, this means that the phase shift between the reflected waves from the two boundaries must be equal, or different by an integer multiple of 2π . Fields that satisfy this condition are called the modes or the eigenfunctions of the waveguide. They maintain the same transverse distribution and polarization at all locations along the waveguide axis [31].

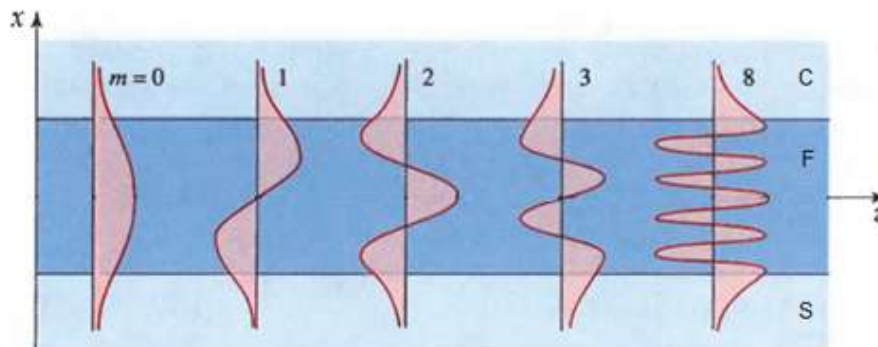


Fig. 5 Field distribution of different modes in a dielectric planar waveguide. Adapted from *Fundamentals of Photonics* (p. 304), by B.E.A. Saleh and M.C. Teich, 2007, New Jersey: John Wiley & Sons. Copyright 2007 by John Wiley & Sons, Inc.

Let's take in consideration a coordinate system where the modes propagate in the z axis, while the x and y axis are perpendicular and parallel to the planar waveguide interfaces, respectively, as shown in **Error! Reference source not found..** The plane wave solutions of Maxwell equations for this waveguide show that only transverse electric (TE) or transverse magnetic (TM) modes can be excited. The boundary conditions of wave propagation in planar waveguides [30], imply that the wavevector of original, refracted and reflected waves must lie in a plane, and also the tangential component of the wavevector across an interface should be continuous. The effective refractive index N , ($n_C < N < n_F$), for planar waveguides is defined as $N = |\vec{k}_t|/|\vec{k}|$, where $|\vec{k}_t| = \beta$ is the tangential component of the wavevector \vec{k} , or the propagation constant [32].

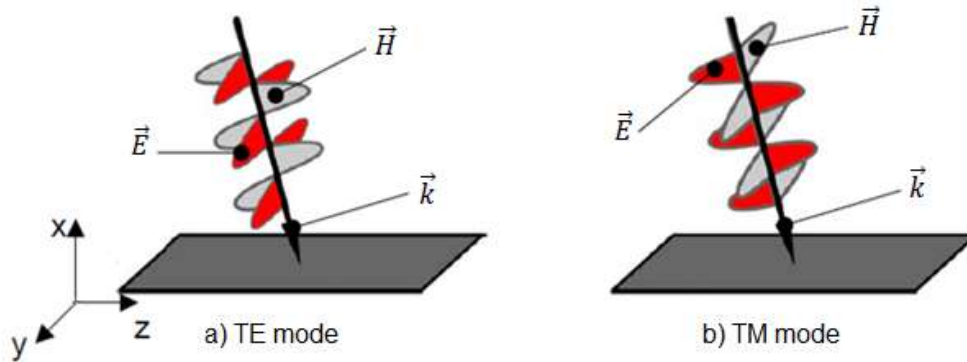


Fig 6. Visualization of a) TE mode and b) TM mode. In planar optical waveguides either the total electric or the total magnetic field can oscillate in the plane of the interfaces.

In case of TE polarization there is no electric field in the direction of beam propagation. In this case the boundary conditions are:

$$\text{TE:} \quad E_x = 0, E_z = 0, H_y = 0, k_y = 0 \text{ thus } E_y, H_z, \frac{\partial E_y}{\partial x} \text{ are continuous.} \quad (2.1a)$$

In case of TM polarization there is no magnetic field in the direction of beam propagation. In this case the boundary conditions are:

$$\text{TM:} \quad E_y = 0, H_x = 0, H_z = 0, k_y = 0 \text{ thus } E_x, H_y, \frac{\partial H_y}{\partial x} \text{ are continuous.} \quad (2.4b)$$

The minimum thickness of the waveguide film for which at least one mode can be guided is known as the “cut-off” thickness of the waveguide, [33]. For TE and TM polarization the “cut-off” thickness is calculated as [34]:

$$(d_F)_m^\rho = \frac{1}{2} \lambda (n_F^2 - n_S^2)^{-1/2} \times \left[m + \pi^{-1} \arctan \left\{ \left(\frac{n_F}{n_C} \right)^{2\rho} \left[\frac{(n_S^2 - n_C^2)}{(n_F^2 - n_S^2)} \right]^{1/2} \right\} \right] \quad (2.5)$$

where $\rho=0$ for TE modes and $\rho=1$ for TM modes. In the field of biosensing, it is of general interest to build waveguides with high optical sensitivity constants. This waveguides usually have a very thin film with high refractive index. It is shown that a waveguide with a very small “cut-off” thickness can be achieved if the difference between the refractive indices of the film and the substrate is approximately $n_F - n_S \geq 0.3$ [34].

The total electromagnetic field propagating inside a waveguide can be given as a linear combination of an upward $E^+(x,z,t)$, and downward $E^-(x,z,t)$, propagating wave, as shown in **Error! Reference source not found.** [32]. In case of a TE field we can write:

$$E(x,z,t) = E^+(x,z,t) + E^-(x,z,t) = (E_0^+ e^{ik_x(x-x_0)+\varphi^+} + E_0^- e^{-ik_x(x-x_0)+\varphi^-}) e^{iNk_0z - i\omega t} \quad (2.6)$$

where E_0 is the amplitude, k_x the wavenumber component in the x direction, while φ^+ and φ^- are the initial phase of the upward and downward propagating waves, respectively. We could write the same for a transverse magnetic (TM) field by substituting E with H .

Outside the waveguide film the amplitude of the propagating wave attenuates exponentially with the distance from the interface, forming the *evanescent wave*. Its penetration depth in the cover medium is the distance at which the field decays by a factor of $1/e$ and can be calculated by [32]:

$$\delta_e = \lambda / \left(2\pi \sqrt{N^2 - n_C^2} \right) \quad (2.7)$$

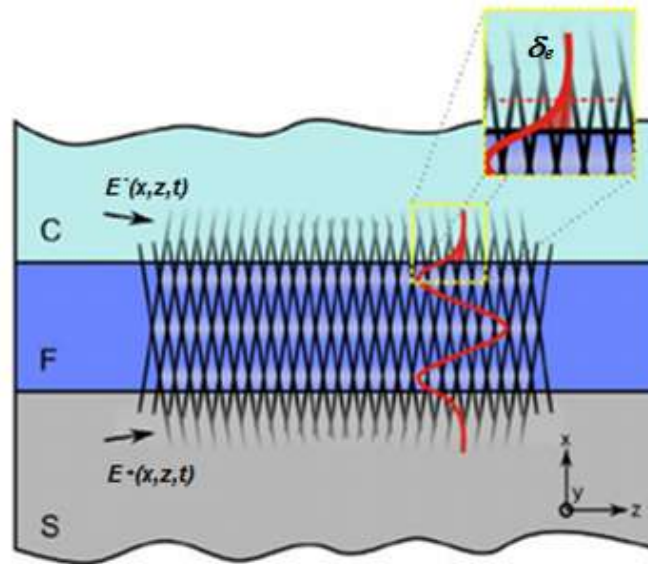


Fig. 7 Visualizaton of mode formation in a planar optical waveguide. The total electromagnetic field inside the waveguide film is composed by the superposition of an upwards $E^+(x, z, t)$ and a downward $E^-(x, z, t)$ propagating wave. Adapted from “Integrated planar optical waveguide interferometer biosensors: A comparative review” by P. Kozma, F. Kehl, E. Förster, C. Stamm, F.F. Bier, 2014, *Biosensors and Bioelectronics*, 58, p. 293. Copyright 2014 by Elsevier B.V.

We can calculate the Fresnel reflection coefficients, r_s and r_c , for the substrate and cover, as follows [35]:

$$r_s = \frac{E_0^+}{E_0^-} = |r_s|e^{i\varphi_s} \quad (2.8a)$$

$$r_c = \frac{E_0^- e^{-ik_x d_F}}{E_0^+ e^{ik_x d_F}} = |r_c|e^{i\varphi_c} \quad (2.8b)$$

where φ_s and φ_c are the phase shifts due to reflection from the substrate and cover, respectively. These phase shifts are different for TE and TM modes therefore they propagate under different conditions. Inserting Eq. (2.8a) into Eq. (2.8b), the mode equation becomes:

$$r_s r_c e^{2ik_x d_F} = |r_s||r_c|e^{i(\varphi_s + \varphi_c + 2k_x d_F)} = 1 \quad (2.9)$$

The solution of Eq. 2.9 defines the *transverse resonance* condition of the guided modes:

$$2k_x d_F - \varphi_s - \varphi_c = 2\pi m \quad (2.10)$$

where m is the mode order.

Although the critical angle, θ_c , does not depend on the polarization of the wave, the phase shifts, φ_s and φ_c , caused by the internal reflection at a given angle depend on the polarization. Therefore, TE and TM waves have different solutions for the transverse resonance condition. For a given polarization, the solution of the transverse resonance condition yields a smaller value of θ and correspondingly a smaller value of β for a larger value of m . Therefore, higher order modes travel with a smaller propagation constant than lower order modes, $\beta_0 > \beta_1 > \beta_2 > \dots$. Only discrete values of $\theta = \theta_m$ can satisfy the resonance condition, because m can assume only integer values. This results in discrete values of the propagation constant, β_m , for the guided modes. The guided mode with $m = 0$ is called the fundamental mode and those with $m = 1, 2, \dots$ are higher-order modes. Because we are considering an asymmetric waveguide where $n_c < n_f > n_s$, the TE and TM fields have unequal amplitudes and decay at different rates at the two boundaries [36]. If the thickness of the waveguide and refractive index contrast between the film and the surroundings is increased, the number of guided modes is also increased; on the other hand the increase of the wavelength decreases the number of guided modes [31].

Error! Reference source not found. depicts the field-distribution profiles of the first four modes, i.e. TE₀, TM₀, TE₁ and TM₁ in planar optical waveguides. When only the fundamental modes are supported, the waveguide is called single-mode [31]. A typical dielectric single-mode waveguide thickness is about 100-200 nm.

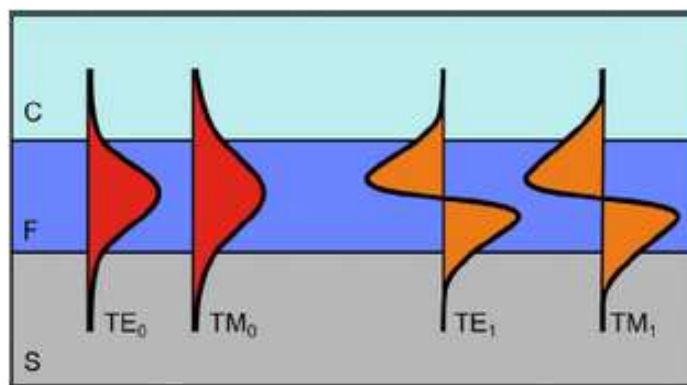


Fig. 8 Schematic visualization of the waveguide modes in a planar optical waveguide. The field-distribution profile of the modes for TE and TM polarization are presented. As it is depicted, TM modes penetrate deeper into the surrounding media than TE modes.

2.4. Sensing with the evanescent field

The main problem of the sensors today is the low interaction between the evanescent field and the measurand. This interaction is proportional to the evanescent field penetration depth in the cladding, which has an upper limit of 100–150 nm. For this reason, the monitoring of biomolecular binding events has been focused near the sensor surface not exceeding this distance. To overcome this limit, the *reverse symmetry* configuration was recently proposed [37]. The reverse configuration offers deeper penetration of the evanescent electromagnetic field into the cover medium, theoretically permitting higher sensitivity to analytes compared to traditional waveguide designs. By introducing a low-refractive-index layer between the substrate and the film the probing distance of the evanescent field can be increased to about 1 μm . This increases the effective area of detection and can detect refractive index changes deep inside the cells and far from the surface. This directly contributes to the increase of sensitivity but is a drawback to specificity because it detects other particles present in the analyte [38]. A large penetration depth can also be obtained for small substrate refractive indices and thin films with high refractive indices [39]. Large film thicknesses lead to a small penetration depth. In this case the effective refractive index, N , will approximately reach the value of the film refractive index, $N \approx n_F$. In case of SPR sensors there is a limited possibility in varying the penetration depth because it is limited to a range of about 180 – 230 nm. Due to the limited penetration depth the disturbing effect of unwanted variations of the bulk refractive index is 2 – 3 times higher compared to IO sensors [39]

In waveguide based sensors the evanescent field is used for sensing binding events in an analyte in close proximity to the surface. When a binding event happens, it changes the refractive index in the near-interface region, which in turn changes the effective refractive index, N . This has an effect on the wavelength of the guided light causing a phase shift relative to a reference beam. For an interaction length, L , the phase shift difference induced in the guided mode due to any refractive index change in the sensing region can be measured as:

$$\Delta\Phi = \frac{\partial\Phi}{\partial N} \frac{\partial N}{\partial n_c} \Delta n_c + \frac{\partial\Phi}{\partial N} \frac{\partial N}{\partial d_A} \Delta d_A = k_0 L S_C \Delta n_c + k_0 L S_A \Delta d_A \quad (2.11)$$

where $S_C = \partial N / \partial n_c$ is the sensitivity to cover refractive index changes and $S_A = \partial N / \partial d_A$ is the sensitivity to adlayer thickness change [40]. By fine tuning the opto-geometrical parameters of the waveguide configuration the values of S_C and S_A can be maximized. The use of integrated optical waveguides in biosensing brings a great advantage due to the flexibility that they offer in choosing different materials and designing structures [41].

An important parameter used in biosensor applications is the adsorption of molecules on the sensor surface. It is very useful to quantify an experiment and is usually measured in mass per unit area. It is called surface mass density, Γ , of a protein adlayer and can be calculated using De Feijter's formula:

$$\Gamma = d_A \frac{n_A - n_c}{\partial n / \partial c} \quad (2.12)$$

where n_A is the adlayer refractive index and $\partial n / \partial c$ is the derivative of solution refractive index with respect to protein concentration [42].

Another important parameter in biosensing which creates the possibility to simply and objectively compare the different existing biosensor configurations is the *Detection Limit* (DL). It is defined as the smallest parameter change that can be detected with reasonable certainty in a configuration. In accordance with the confidence level needed, a confidence factor k is defined. A general formula to calculate the DL is [43]:

$$DL = k \frac{\sigma}{S} \tag{2.13}$$

where σ is the standard deviation of the blank signal and S the sensitivity. In biosensorics, k is generally chosen 3, because it gives a 0.13% chance that a signal measured at the limit of detection would be the result of random fluctuation of the signal, and not a meaningful change. In optical label-free sensors there are typically three ways to specify the DL. The first is to specify it in refractive index units (RIU) since these sensors are sensitive to the RI change in bulk solution. This gives the possibility to make a rough comparison of the sensing capability among different optical technologies and structures. The second way is to use surface mass density (or total mass) in units of $\text{pg}\cdot\text{mm}^{-2}$. It reflects the intrinsic detection capability of a sensor and can be used to evaluate or compare the sensor performance. The drawback is that experimentally it is difficult to determine surface mass density accurately. The third way is to use sample concentration (in units of $\text{ng}\cdot\text{ml}^{-1}$ or molarity). It is easy to determine from an experiment as no detailed information regarding the mass density on the surface is needed. These three DLs are correlated and the relationship between them needs to be studied for each individual optical biosensor [12].

2.5 Waveguide types

Today, there are various configurations in material and geometry of planar optical waveguides. Depending on their geometrical design they can be classified in two main types: 1) slab waveguides and 2) channel waveguides [44]. Slab waveguides have a planar geometry and guide light only in the transverse direction. [45]. They are easy to fabricate and there is no scattering between the transverse and lateral modes. Channel waveguides offer two dimensional optical confinement and act as a pipe for guiding the light. They exist in different configurations as shown in **Error! Reference source not found.**; buried, diffused, ridge, rib, strip-loaded, and ARROW waveguides [29]. A buried waveguide is imprinted in the substrate and completely surrounded by the cladding material. Therefore, it is suitable for guiding the light but not a convenient configuration for the sensitive area of a biosensor.

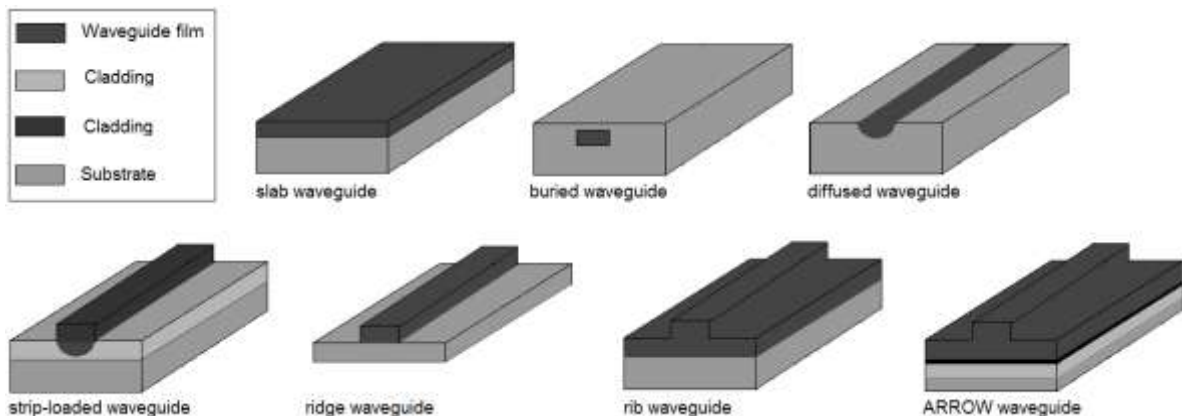


Fig 9. Schematic 3-dimensional representation of different waveguide types. The same functional layers are marked with the same colours.

In case of the *diffused waveguide* the high-index region in the substrate is formed through diffusion of dopants, such as *Ti*, or by ion exchange. Due to the diffusion process, the film boundaries in the substrate are not sharply defined [46]. A *strip-loaded waveguide* is formed by loading a planar waveguide, which already provides optical confinement in the transverse direction, with a dielectric or a metal strip to facilitate optical confinement in the lateral direction. The waveguiding film of this waveguide is the region under the loaded strip, with its width determined by the width of the loaded strip. Again this configuration is not suitable for biosensing due to the shielding of the film [36].

A *ridge waveguide* has a structure similar to the strip waveguide, but the ridge in this case is actually the waveguiding film. A ridge waveguide has a strong optical confinement because it is surrounded on the three sides by low-index material (air, substrate or cladding).

In case of the *rib waveguide*, the strip or the ridge has the same refractive index as the high index planar layer beneath it and is part of the waveguiding film. The ridge and rib waveguide are very common in the field of optical planar waveguide biosensors [47]. The *Anti-Resonant Reflecting Optical Waveguide* (ARROW) is an alternative to the rib waveguide configuration. The light is guided in the waveguide rib due to the total internal reflection at the air-film interface and the high anti-resonant reflection (>99.9%) from the interference cladding

layers, which behave as Fabry-Perot resonators operating at their antiresonant wavelengths. They separate the waveguide film from the substrate and have an effective single-mode behavior. They present low losses for the fundamental mode and filter out higher order modes by loss discrimination. Compared to the total internal reflection waveguides ARROW waveguides offer larger film thickness, greater parameter tolerance in fabrication and lower losses [48, 49]. Both slab and channel waveguides can be divided in step-index, graded index and photonic crystal waveguides, depending on their refractive index profile. When the refractive index exhibits abrupt changes between the waveguide film and the cladding it is called a *step-index waveguide*, while when the refractive index varies gradually and has a smooth transition to the cover or substrate, it is called a *graded-index waveguide*. The most common materials used to form the thin layer of high refractive index in step-index waveguides are Ta₂O₅, TiO₂, Si₃N₄, Al₂O₃ or SiON [50, 51]. Graded-index waveguides can be fabricated by implementing both light and heavy ions, with the combination of other techniques as photolithography, etching and ion exchange. Good quality graded-index waveguides can be fabricated in glass by femtosecond laser pulses [52, 53]. The high contrast in refractive index that is achieved in step-index waveguides ensures good guidance conditions and optimizes the evanescent field distribution in the film-cover interface compared to graded-index waveguides, therefore they offer better sensitivity [54]. **Error! Reference source not found.** shows refractive index variations in step-index and graded-index waveguides.

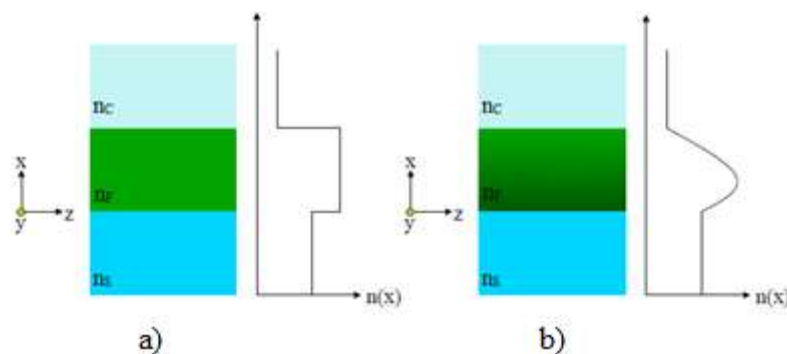


Fig. 10. a) Step-index and b) graded-index waveguide. Step-index waveguides exhibit an abrupt refractive index step at the substrate and cover transitions, while the refractive index profile of graded-index waveguides has a smooth transition between them.

2.6 Light Coupling Techniques in Waveguides

In order for the light to be guided in a waveguide it first needs to be coupled in it from an external source. The five main coupling techniques used with planar waveguides are: a) end-fire-, b) butt-end-, c) prism-, d) grating and e) directional coupling, as depicted in **Error! Reference source not found.** [31, 55]. In *end-fire coupling* the light is directly focused on a cleaved end face of the waveguide. This is the simplest way to couple a free-space source into a waveguide, but on the other side it has some drawbacks as it needs a very precise alignment of the incident light relative to the waveguide due to the small dimensions of the waveguide slab. Focusing and alignment in this case are usually difficult and coupling efficiency is low especially in thin single-mode waveguides. For efficient coupling the transverse distribution and the polarization of the incident light must match that of the desired mode and the numerical aperture of the focusing lens needs to be fitted to the propagation constant of the mode excited in the waveguide.

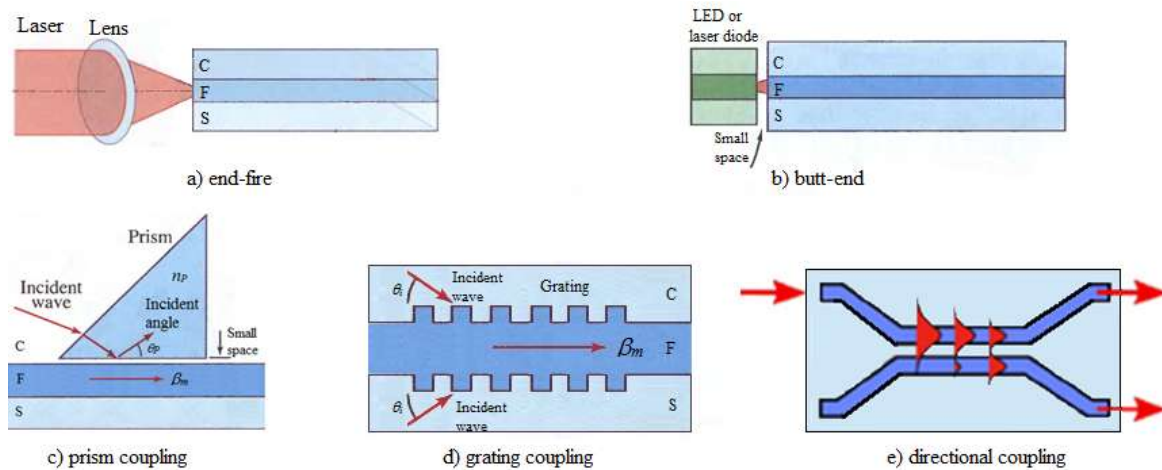


Fig. 11. Light coupling techniques for optical waveguides a) end-fire coupling, (b) butt-end coupling c) prism coupling, d) grating coupling and (e) directional coupling

The *butt-end coupling* is a closely related concept to free space end-fire coupling. It couples the light from a semiconductor source such as a light-emitting diode or a laser diode, or by bringing in contact an optical fiber with the cleaved end face of a waveguide, leaving a small space between the two physical units for maximum coupling. Similarly to end-fire coupling, the alignment is crucial as well as the mode matching between them. It is generally easier than the alignment of a light cone as in the case of end-fire coupling (especially for wavelengths beyond the visible spectrum), and can be done under a microscope [56]. When a prism with a high refractive index is used to couple the light into the waveguide film, the method is called *prism coupling*. The prism is either placed at a short distance from the waveguide or is brought in direct contact with it by applying mechanical pressure or by the use of immersion oil. The incident wave is refracted into the prism and undergoes total internal reflection at an angle θ_p . The incident and reflected waves form a wave traveling in the z direction with a propagation constant $\beta_p = n_p k_0 \cos \theta$, where n_p is the refractive index of the prism. In the space separating the prism and the slab waveguide extends the exponentially decaying evanescent wave of the field traveling into the prism. If the distance between the prism and the waveguide is sufficiently small, the wave is coupled into a mode of the slab waveguide with a matching propagation constant $\beta_m \approx \beta_p = n_p k_c \cos \theta_p$, where k_c is the wavenumber of the cover medium. This method offers high efficiency not only for coupling the light into the waveguide but also for extracting it. Due to the mechanical pressure or immersion oil applied when in direct contact with the waveguide, this method is not convenient for sensing applications because the applied pressure can lead to slight waveguide deformations, whereas the immersion oil may contaminate the waveguide surface [57].

Waveguide grating couplers have a periodic alternating effective refractive index, usually in the range of the wavelength [58, 59]. The grating coupler consists of a periodically corrugated surface, realized by embossing or photolithographic processes or an alternating modification of the waveguide refractive index. The modification of the refractive index can be achieved by ion exchange or UV induced refractive index modulation [60]. The phase-matching condition in grating couplers is achieved due to the phase modulation of the incident wave from the periodic structure of the grating coupler. A grating with period A modulates the incoming wave by a phase factor $2\pi q/Az$, where $q = \pm 1, \pm 2, \dots$. This is equivalent in changing the z component of the wavevector by a factor $2\pi q/A$. The phase matching condition can now be written as $\beta_m = n_c k_c \cos \theta_i + 2\pi q/A$, where θ_i is the incident angle, while n_c and k_c are the refractive index and wavenumber of the cover medium, respectively [61]. This technique has various advantages compared to the other mentioned methods: a) The fact that only the coupling angle on the incident beam needs to be adjusted in order to achieve the phase-matching condition, makes this coupling technique rather easy to implement. b) Contrary to the prism coupler light can be coupled via the substrate, besides via the cover. This eliminates the problem that exists in prism coupling configuration, where light is obstructed from fluidic chamber placed on the cover of the waveguide. Additionally, no immersion oil is needed in this configuration. The main drawbacks are that the production of the waveguide gratings is technology-intensive, and they are very sensitive to mechanical vibrations, since the coupling efficiency is very sensitive to the angle of incidence [62].

In directional coupling a mode is excited in a channel waveguide via the evanescent field of another waveguide in close proximity with the first one [63]. In other words, one of the waveguides acts as the source for the other, and the amount of optical power that can be transferred between them is related to some geometrical parameters such as interaction length and their relative interdistance. In general, the length of the waveguides in close proximity necessary to transfer the power completely for one waveguide to another is

called *coupling length*, L_0 , or the *transfer distance*. At half of the distance, $L_0/2$, half of the power is transferred and the device is called a 3-dB coupler, i.e a 50/50 beam splitter. Directional coupling is mainly used in signal multiplexing or for coupling light into ring resonators, where this mechanism is necessary. Similar to grating coupling this method has the disadvantage that is technology-intensive, and analog to butt-end coupling the light needs to be previously coupled into one of the waveguides.

III. Conclusions

After a short presentation of the theory behind the working principle of interferometer biosensors, were presented some of the most important parameters to be taken in consideration. The combination of planar waveguides with interferometry techniques to realize detection of analytes in a sample, led to the realization of multiple configurations for the biosensors without labels, with very good characteristics and detection limits compared to other sensing devices. As shown in this review, interferometric biosensor abilities have dynamically improved during the last 20 years. Nowadays, it is possible with these devices to detect the presence of even small molecules that are deposited or connected onto a sensing surface. As it is shown, nowadays is achieved a detection limit of 0.1 pg/mm^2 [64].

Nevertheless, from the technological point of view there are some problems to be solved in order for these devices to be considered portable and usable maybe from the patient himself. The need for coherent quality light sources, which are still big and require a lot of power, stabilized coupling of light, an efficient cancellation of electrical and mechanical noises, and an efficient control of temperature in order to reduce measurement noise, make this configurations difficult to be completely integrated into portable devices.

References

- [1]. Updike, S. and G. Hicks, *The enzyme electrode*. Nature, 1967. **214**: p. 986-988.
- [2]. Chambers, J.P., et al., *Biosensor recognition elements*. 2008, DTIC Document.
- [3]. Oliver, N., et al., *Glucose sensors: a review of current and emerging technology*. Diabetic Medicine, 2009. **26**(3): p. 197-210.
- [4]. Holford, T.R., F. Davis, and S.P. Higson, *Recent trends in antibody based sensors*. Biosensors and Bioelectronics, 2012. **34**(1): p. 12-24.
- [5]. Lazcka, O., F.J. Del Campo, and F.X. Munoz, *Pathogen detection: A perspective of traditional methods and biosensors*. Biosensors and Bioelectronics, 2007. **22**(7): p. 1205-1217.
- [6]. O'Malley, S., *Recent advances in label-free biosensors applications in protein biosynthesis and hts screening*. Protein Biosynthesis (TE Esterhouse and LB Petrinis, eds.), Nova Science Publishers, Inc, 2008.
- [7]. Cunningham, B.T., *Label-free optical biosensors: An introduction*. Label-Free Biosensors: Techniques and Applications, 2009: p. 1.
- [8]. Justino, C.I., T.A. Rocha-Santos, and A.C. Duarte, *Review of analytical figures of merit of sensors and biosensors in clinical applications*. TrAC Trends in Analytical Chemistry, 2010. **29**(10): p. 1172-1183.
- [9]. Alivisatos, A.P., *Less is more in medicine*. Sci Am, 2001. **285**(3): p. 66-73.
- [10]. Jain, K.K., *Nanotechnology in clinical laboratory diagnostics*. Clinica Chimica Acta, 2005. **358**(1): p. 37-54.
- [11]. Cooper, M.A., *Optical biosensors in drug discovery*. Nature Reviews Drug Discovery, 2002. **1**(7): p. 515-528.
- [12]. Fan, X., et al., *Sensitive optical biosensors for unlabeled targets: A review*. analytica chimica acta, 2008. **620**(1): p. 8-26.
- [13]. Estevez, M.-C., M. Alvarez, and L.M. Lechuga, *Integrated optical devices for lab-on-a-chip biosensing applications*. Laser & Photonics Reviews, 2012. **6**(4): p. 463-487.
- [14]. Duval, D., et al. *Interferometric waveguide biosensors based on Si-technology for point-of-care diagnostic*. in *SPIE Photonics Europe*. 2012a. International Society for Optics and Photonics.
- [15]. Young, T., *The Bakerian Lecture: Experiments and Calculations Relative to Physical Optics*. Philosophical Transactions of the Royal Society of London, 1804. **94**: p. 1-16.
- [16]. Zourob, M., S. Elwary, and A.P. Turner, *Principles of Bacterial Detection: Biosensors, Recognition Receptors and Microsystems: Biosensors, Recognition Receptors, and Microsystems*. 2008: Springer Science & Business Media.
- [17]. Bell, E., *Measurement of the far infrared optical properties of solids with a michelson interferometer used in the asymmetric mode: Part I, mathematical formulation**. Infrared Physics, 1966. **6**(2): p. 57-74.
- [18]. Hariharan, P., *Basics of interferometry*. 2010: Academic Press.
- [19]. Campbell, D.P., *Interferometric biosensors*, in *Principles of Bacterial Detection: Biosensors, Recognition Receptors and Microsystems*. 2008, Springer. p. 169-211.
- [20]. Brandenburg, A. and R. Henninger, *Integrated optical Young interferometer*. Applied optics, 1994. **33**(25): p. 5941-5947.
- [21]. Mach, L., *Über einen interferenzrefraktor*. Z. für Instrumentenkunde, 1892. **12**: p. 89-93.
- [22]. Jenkins, F.A. and H.E. White, *Fundamentals of optics*. 1957a: McGraw-Hill.
- [23]. Jenkins, F.A. and H.E. White, *The Double Slit*. 1957b, McGraw-Hill. p. 311-327.
- [24]. Heideman, R. and P. Lambeck, *Remote opto-chemical sensing with extreme sensitivity: design, fabrication and performance of a pigtailed integrated optical phase-modulated Mach-Zehnder interferometer system*. Sensors and Actuators B: Chemical, 1999. **61**(1): p. 100-127.
- [25]. Ymeti, A., et al., *Fast, ultrasensitive virus detection using a Young interferometer sensor*. Nano Letters, 2007. **7**(2): p. 394-397.
- [26]. Khoxhi, M., et al., *Multimode Interference Biosensor Working With Multiple Wavelengths And Two Polarizations*. International Journal of Scientific & Technology Research (IJSTR), 2014. **3**(7): p. 314-320
- [27]. Colladon, D., *Comptes rendus de l'Académie des Sciences 1842*. **15**: p. 800-802.
- [28]. Hecht, J., *City of Light: The Story of Fiber Optics*. 1999: Oxford University Press, USA.
- [29]. Anderson, D.B., *Optical and Electro-optical Information Processing*. 1965: MIT Press.
- [30]. Jackson, J.D., *Classical electrodynamics*. 1998a, Wiley & Sons. p. 295-351.
- [31]. Saleh, B.E.A. and M.C. Teich, *Fundamentals of Photonics*. 2007: Wiley.
- [32]. Cottier, K., *Advanced Label-free Biochemical Sensors Based on Integrated Optical Waveguide Gratings: Theory, Modeling, Design and Characterization*. 2004: UFO, Atelier für Gestaltung und Verlag.
- [33]. Jackson, J.D., *Classical electrodynamics*. 1998b, Wiley & Sons. p. 352-406.

- [34]. Lukosz, W., *Integrated optical chemical and direct biochemical sensors*. Sensors and Actuators B: Chemical, 1995. **29**(1): p. 37-50.
- [35]. Takada, K., et al., *New measurement system for fault location in optical waveguide devices based on an interferometric technique*. Applied optics, 1987. **26**(9): p. 1603-1606.
- [36]. Liu, J., *Photonic Devices*. 2005: Cambridge University Press.
- [37]. Horváth, R., L.R. Lindvold, and N.B. Larsen, *Reverse-symmetry waveguides: theory and fabrication*. Applied Physics B, 2002. **74**(4-5): p. 383-393.
- [38]. Horvath, R., et al., *Monitoring of living cell attachment and spreading using reverse symmetry waveguide sensing*. Applied Physics Letters, 2005. **86**(7): p. 071101.
- [39]. Kunz, R. and K. Cottier, *Optimizing integrated optical chips for label-free (bio-) chemical sensing*. Analytical and bioanalytical chemistry, 2006. **384**(1): p. 180-190.
- [40]. Guillod, T., F. Kehl, and C.V. Hafner, *FEM-based method for the simulation of dielectric waveguide grating biosensors*. Progress In Electromagnetics Research, 2013. **137**: p. 565-583.
- [41]. Lambeck, P.V., *Integrated optical sensors for the chemical domain*. Measurement science and technology, 2006. **17**(8): p. R93.
- [42]. De Feijter, J., d.J. Benjamins, and F. Veer, *Ellipsometry as a tool to study the adsorption behavior of synthetic and biopolymers at the air-water interface*. Biopolymers, 1978. **17**(7): p. 1759-1772.
- [43]. Long, G.L. and J.D. Winefordner, *Limit of detection. A closer look at the IUPAC definition*. Analytical Chemistry, 1983. **55**(7): p. 712A-724A.
- [44]. Campbell, D., *Interferometric Biosensors*, in *Principles of Bacterial Detection: Biosensors, Recognition Receptors and Microsystems*, M. Zourob, S. Elwary, and A. Turner, Editors. 2008, Springer New York. p. 169-211.
- [45]. Snyder, A.W. and J. Love, *Optical waveguide theory*. Vol. 190. 1983: Springer Science & Business Media.
- [46]. Burns, W., et al., *Ti diffusion in Ti: LiNbO₃ planar and channel optical waveguides*. Journal of Applied Physics, 1979. **50**(10): p. 6175-6182.
- [47]. Agrawal, G.P., *Optical Waveguides (OPT568)*. Institute of Optics, University of Rochester, 2007.
- [48]. Benaissa, K. and A. Nathan, *Silicon anti-resonant reflecting optical waveguides for sensor applications*. Sensors and Actuators A: Physical, 1998. **65**(1): p. 33-44.
- [49]. Prieto, F., et al., *Design and analysis of silicon antiresonant reflecting optical waveguides for evanescent field sensor*. Journal of lightwave technology, 2000. **18**(7): p. 966.
- [50]. Brecht, A. and G. Gauglitz, *Optical probes and transducers*. Biosensors and Bioelectronics, 1995. **10**(9): p. 923-936.
- [51]. Salemink, H.W.M., et al., *Silicon-Oxynitride (SiON) for Photonic Integrated Circuits*. MRS Online Proceedings Library, 1999. **574**: p. null-null.
- [52]. Chen, F., X.-L. Wang, and K.-M. Wang, *Development of ion-implanted optical waveguides in optical materials: A review*. Optical materials, 2007. **29**(11): p. 1523-1542.
- [53]. Davis, K.M., et al., *Writing waveguides in glass with a femtosecond laser*. Optics letters, 1996. **21**(21): p. 1729-1731.
- [54]. Parriaux, O. and G. Veldhuis, *Normalized analysis for the sensitivity optimization of integrated optical evanescent-wave sensors*. Journal of lightwave technology, 1998. **16**(4): p. 573.
- [55]. Tamir, T., *Beam and Waveguide Couplers*, in *Integrated Optics*, T. Tamir, Editor. 1975, Springer Berlin Heidelberg. p. 83-137.
- [56]. Korvink, J. and O. Paul, *MEMS: A practical guide of design, analysis, and applications*. 2010, Springer Science & Business Media. p. 457-458.
- [57]. Assanto, G., et al., *Prism coupling into ZnS waveguides: a classic example of a nonlinear coupler*. Optics letters, 1986. **11**(10): p. 644-646.
- [58]. Dakss, M., et al., *Grating coupler for efficient excitation of optical guided waves in thin films*. Applied physics letters, 1970. **16**(12): p. 523-525.
- [59]. Peng, S., T. Tamir, and H.L. Bertoni, *Theory of periodic dielectric waveguides*. Microwave Theory and Techniques, IEEE Transactions on, 1975. **23**(1): p. 123-133.
- [60]. Hamori, A. and N. Nagy, *Sub-micrometer period refractive index grating coupler for single mode optical waveguide sensors [chemical and biosensor applications]*. in *Sensors, 2004. Proceedings of IEEE*. 2004. IEEE.
- [61]. Tamir, T. and S.-T. Peng, *Analysis and design of grating couplers*. Applied physics, 1977. **14**(3): p. 235-254.
- [62]. Vörös, J., et al., *Optical grating coupler biosensors*. Biomaterials, 2002. **23**(17): p. 3699-3710.
- [63]. Marcatili, E.A., *Dielectric rectangular waveguide and directional coupler for integrated optics*. Bell System Technical Journal, 1969. **48**(7): p. 2071-2102.
- [64]. Ronan, G., *Doubling Up*. SPIES oemagazine (Sep. 2004), 2004: p. 17-20.